ARTICLE IN PRESS

Journal of Computational and Applied Mathematics xxx (xxxx) xxx

Contents lists available at ScienceDirect

Journal of Computational and Applied Mathematics

journal homepage: www.elsevier.com/locate/cam

Study of boundary conditions in the Iterative Filtering method for the decomposition of nonstationary signals

Antonio Cicone [a,b,c], Pietro Dell'Acqua [d,*]

[a] Istituto Nazionale di Alta Matematica, Città Universitaria, P.le Aldo Moro 5, 00185 Roma, Italy
[b] DISIM, Università degli Studi dell'Aquila, via Vetoio 1, 67100 L'Aquila, Italy
[c] Gran Sasso Science Institute, viale Francesco Crispi 7, 67100 L'Aquila, Italy
[d] Libera Università di Bolzano, Piazza Domenicani 3, 39100 Bolzano, Italy

ARTICLE INFO

Article history:
Received 30 December 2018
Received in revised form 16 April 2019

MSC:
65F15
15A18
15B05
15B51
94A12
65F99

Keywords:
Signal decomposition
Boundary conditions
Structured matrices
Iterative filtering
Empirical mode decomposition
Nonstationary signal

ABSTRACT

Nonstationary and non-linear signals are ubiquitous in real life. Their decomposition and analysis is an important research topic of signal processing. Recently a new technique, called Iterative Filtering, has been developed with the goal of decomposing such signals into simple oscillatory components. Several papers have been devoted to the investigation of this technique from a mathematical point of view. All these works start with the assumption that each compactly supported signal is extended periodically outside the boundaries. In this work, we tackle the problem of studying the influence of different boundary conditions on the decompositions produced by the Iterative Filtering method. In particular, the choice of boundary conditions gives rise to different types of structured matrices. Thus, we describe their spectral properties and the convergence properties of Iterative Filtering algorithm when such matrices are involved. Numerical results on artificial and real life signals provide interesting insight on important aspects such as accuracy and error propagation of the proposed technique and pave the way for further promising developments.

1. Introduction

Given a real life nonstationary signal $\mathbf{s}(x)$, $x \in \mathbb{R}$, we may be interested in decomposing it into simple components in order to identify features and quasi periodicities hidden in it. We can think, for instance, to a economic index, like the GDP of a nation, or a geophysical signal, like the sea level during a tsunami, as well as to an engineering measure, like the vibrations of a structure or machinery. Standard techniques, like Fourier or wavelet transform, cannot help, in general, to decompose meaningfully nonstationary signals. Whereas, following the idea proposed by Huang et al. in [1], we can iteratively decompose such signals into a finite sequence of simple components, defined Intrinsic Mode Functions (IMFs), which fulfill two properties: (*i*) the number of extrema and the number of zero crossings must either equal or differ at most by one; (*ii*) considering upper and lower envelopes connecting respectively all the local maxima and minima of the function, their mean has to be zero at any point.

The method originally proposed by Huang et al. in [1] to decompose a signal into IMFs, called Empirical Mode Decomposition (EMD), proved to be unstable to small perturbations. For this reason an alternative algorithm, called

* Corresponding author.
E-mail addresses: antonio.cicone@univaq.it (A. Cicone), pietro.dellacqua@gmail.com (P. Dell'Acqua).

https://doi.org/10.1016/j.cam.2019.04.028
0377-0427/

Ensemble Empirical Mode Decomposition (EEMD), was proposed in [2]. EEMD is based on the idea of applying EMD to an ensemble of signals produced perturbing hundreds of times the given one with random noise. The decomposition is then derived as the average decomposition of the ensemble. In [3] the authors proposed an alternative technique to the EMD, called Iterative Filtering (IF), which has the very same structure of EMD, but it is stable and convergent both in the continuous [4,5] and in the discrete setting [6–10]. We point out that IF has been also generalized producing the so called Adaptive Local Iterative Filtering (ALIF) algorithm whose convergence and stability are under investigation [4,11]. For further details on why standard techniques may fail in decomposing a nonstationary signal and the advantages of using EEMD or IF we refer the interested reader to [12].

In this work we consider the case of compactly supported and discrete signals. For simplicity we assume that each signal $\mathbf{s} = \left[\mathbf{s}(x_j)\right]_{j=0}^{n-1}$ (with $n \in \mathbb{N}$) is supported on $[0, 1]$ and it is sampled at n points $x_j = \frac{j}{n-1}$, with $j = 0, \ldots, n-1$. Without losing generality we can further assume that $\|\mathbf{s}\|_2 = 1$.

Any signal decomposition method which deals with a compactly supported signal requires assumptions on how the signal extends outside the boundaries, the so called Boundary Conditions (BCs). This aspect has a key role in many applications, for instance in Finance and Economy as well as in image restoration [13–15], and usually the goal is to employ BCs able to guarantee good accuracy of the approximated solution computed by some numerical algorithm [16,17]. The issue of boundary conditions appears also in the framework of EMD method. In such context, "end effects" are usually treated with basic techniques, for instance using the idea of "window frame" [18,19]. Regarding IF, in [6] the authors addressed its convergence when it is assumed that the signals extend periodically outside the boundaries. The questions which are still open are: does IF converge also for other kinds of BCs? Given a signal extended artificially outside the boundaries in a certain way, how do the errors introduced outside the boundaries effect the decomposition inside the signal in the iterations? Given a compactly supported signal what is the best choice in terms of BCs?

The paper is organized as follows. In Section 2 we review the IF algorithm applied to discrete and compactly supported signals. Section 3 is devoted to a summary of BCs and their properties. In Section 4 we study the IF convergence when different BCs are chosen for the signal. In Section 5 we present an extended version of IF method, which is useful for addressing the question of how the errors propagate from outside the boundaries to the inside as well as for applying generic BCs. This work ends with some numerical examples showing the impact of BCs on decomposition quality and error propagation in Section 6, and concluding remarks.

2. Discrete iterative filtering

In this section we review the IF method focusing on the case of discrete and compactly supported signals $\mathbf{s}$. We start from the definition of filter

Definition 1. A non-negative vector $\mathbf{w} = (0, \ldots, 0, w_{-\ell}, \ldots, w_{-1}, w_0, w_1, \ldots, w_\ell, 0, \ldots, 0) \in \mathbb{R}^n$ such that $w_j > 0$ for $j = -\ell, \ldots, \ell$ and $\sum_{j=-\ell}^{\ell} w_j = 1$ is called a **filter** of length ℓ, with $0 < \ell \leq \lfloor \frac{n-1}{2} \rfloor$. If $w_{-j} = w_j$ for $j = 1, \ldots, \ell$, then $\mathbf{w}$ is called **symmetric**. If $w_i \geq w_j$ for $0 \leq i < j$, and $w_i \geq w_j$ for $j < i \leq 0$, then $\mathbf{w}$ is called **decreasing**.

In this work we consider only symmetric filters. When we have a symmetric filter associated with some step m, we employ the following notation

$$\mathbf{w}_m = (0, \ldots, 0, w^m_{\ell_m}, \ldots, w^m_1, w^m_0, w^m_1, \ldots, w^m_{\ell_m}, 0, \ldots, 0), \tag{1}$$

with $w^m_0 + 2\sum_{j=1}^{\ell_m} w^m_j = 1$.

If we assume that some symmetric filter shape $h : [-1, 1] \to \mathbb{R}^+$ has been selected a priori, like one of the Fokker–Planck filters described in [4], then the elements w^m_j can be computed, for $j = 0, 1, \ldots, \ell_m$, by the linear scaling formula

$$w^m_j = h\left(\frac{j}{\ell_m}\right)\frac{1}{\ell_m}, \tag{2}$$

where $\ell_m > 0$ is the length that characterizes the filter. Assuming $\mathbf{s}^m_1 = \mathbf{s}$, where the two indices will become clear in the next paragraph, the main step of the IF method, for $i = 0, \ldots, n-1$, is

$$\begin{aligned}\mathbf{s}^m_{k+1}(x_i) &= \mathbf{s}^m_k(x_i) - \int_{x_i - \frac{\ell_m}{n-1}}^{x_i + \frac{\ell_m}{n-1}} \mathbf{s}^m_k(y) h\left(\frac{(x_i - y)(n-1)}{\ell_m}\right)\frac{n-1}{\ell_m}\mathrm{d}y \\ &\approx \mathbf{s}^m_k(x_i) - \sum_{x_j = x_i - \frac{\ell_m}{n-1}}^{x_i + \frac{\ell_m}{n-1}} \mathbf{s}^m_k(x_j) h\left(\frac{(x_i - x_j)(n-1)}{\ell_m}\right)\frac{1}{\ell_m}\end{aligned}$$

Please cite this article as: A. Cicone and P. Dell'Acqua, Study of boundary conditions in the Iterative Filtering method for the decomposition of nonstationary signals, Journal of Computational and Applied Mathematics (2019), https://doi.org/10.1016/j.cam.2019.04.028.

$$= \mathbf{s}_k^m(x_i) - \sum_{j=i-\ell_m}^{i+\ell_m} \mathbf{s}_k^m(x_j) h\left(\frac{i-j}{\ell_m}\right)\frac{1}{\ell_m}$$
$$= \mathbf{s}_k^m(x_i) - \sum_{j=i-\ell_m}^{i+\ell_m} \mathbf{s}_k^m(x_j) w_{|i-j|}^m$$

Algorithm 1 provides the pseudocode of the Discrete Iterative Filtering (DIF) Algorithm. We observe that the first while loop is called Outer Loop, whereas the second one Inner Loop. In the notation $\mathbf{s}_k^m$, m denotes the step relative to the Outer Loop, while k denotes the step relative to the Inner Loop. The idea is to suitably choose the filter length ℓ_m in order to capture the desired frequencies in the IMF $\mathbf{f}_m$, and this is done by subtracting iteratively from the signal its moving average computed as convolution of the signal itself with the selected filter. In matrix form we have

$$\mathbf{s}_{k+1}^m = (I - W_m^{\mathcal{BC}})\mathbf{s}_k^m, \tag{3}$$

where $W_m^{\mathcal{BC}}$ is a structured matrix constructed from the filter $\mathbf{w}_m$ and the BCs imposed. In particular $W_m^{\mathcal{BC}}$ can be written as the sum of two matrices

$$W_m^{\mathcal{BC}} = T_m + K_m^{\mathcal{BC}}, \tag{4}$$

where the first one is a Toeplitz matrix, while the second one is a correction matrix which depends on BCs (for details, see Section 3).

Algorithm 1 Discrete Iterative Filtering IMFs = DIF(s, h)

```
m = 1
s_1^m = s
while the number of extrema of s_1^m ≥ 2 do
  k = 1
  compute the filter length ℓ_m for the signal s_k^m
  compute w_m (having h and ℓ_m)
  while the stopping criterion is not satisfied do
    (s_k^m)^BC(x_i) = s_k^m(x_i), i = 0, ..., n − 1
    apply BCs for computing (s_k^m)^BC(x_i), i = −ℓ_m, ..., −1 and i = n, ..., n − 1 + ℓ_m
    s_{k+1}^m(x_i) = s_k^m(x_i) − Σ_{j=i−ℓ_m}^{i+ℓ_m} (s_k^m)^BC(x_j) w_{|i−j|}^m,   i = 0, ..., n − 1
    k = k + 1
  end while
  f_m = s_k^m
  s_1^{m+1} = s_1^m − f_m
  m = m + 1
end while
f_m = s_1^m
IMFs = {f_1, ..., f_m}
```

From (3), it follows immediately that

$$\mathbf{s}_{k+1}^m = (I - W_m^{\mathcal{BC}})^k \mathbf{s}_1^m, \tag{5}$$

so ideally the first IMF is given by

$$\mathbf{f}_1 = \lim_{k\to\infty} (I - W_1^{\mathcal{BC}})^k \mathbf{s}. \tag{6}$$

However, in the implemented algorithm we do not let k to go to infinity, instead we use a stopping criterion. We can define, for instance, the following quantity

$$\Delta_k^m := \frac{\|\mathbf{s}_{k+1}^m - \mathbf{s}_k^m\|_2}{\|\mathbf{s}_k^m\|_2}, \tag{7}$$

so we can either stop the process when the value Δ_k^m reaches a certain threshold or we can introduce a limit on the maximal number of iterations for all the Inner Loops. It is also possible to adopt different stopping criteria for different Inner Loops.

3. Boundary conditions and structured matrices

The DIF algorithm, as any other method that deals with compactly supported signal, requires to extend the signal outside the field of view in which the detection is made. This is what we call the Boundary conditions (BCs) problem. So

Please cite this article as: A. Cicone and P. Dell'Acqua, Study of boundary conditions in the Iterative Filtering method for the decomposition of nonstationary signals, Journal of Computational and Applied Mathematics (2019), https://doi.org/10.1016/j.cam.2019.04.028.

let $\mathbf{s}$ be the signal inside the boundaries and let p be the length of how much we extend the signal outside the boundaries, we have that, for $j = 1, \dots, p$, Zero BCs are defined as

$$\mathbf{s}(x_{-j}) = 0, \qquad \mathbf{s}(x_{n-1+j}) = 0, \tag{8}$$

Periodic BCs are defined as

$$\mathbf{s}(x_{-j}) = \mathbf{s}(x_{n-j}), \qquad \mathbf{s}(x_{n-1+j}) = \mathbf{s}(x_{j-1}), \tag{9}$$

Reflective BCs [20] are defined as

$$\mathbf{s}(x_{-j}) = \mathbf{s}(x_{j-1}), \qquad \mathbf{s}(x_{n-1+j}) = \mathbf{s}_{n-j}, \tag{10}$$

Anti-Reflective BCs [21] are defined as

$$\mathbf{s}(x_{-j}) = 2\mathbf{s}(x_0) - \mathbf{s}(x_j), \qquad \mathbf{s}(x_{n-1+j}) = 2\mathbf{s}(x_{n-1}) - \mathbf{s}(x_{n-1-j}). \tag{11}$$

According to the BCs imposed, we have a different kind of structured matrix $W^{\mathcal{BC}}$ in (4), whose elements are defined based on the values of the filter $\mathbf{w}$ of length ℓ. As said, here we take into account symmetric filters, since this choice allows to have useful theoretical properties. In particular, symmetry is not necessary to get the algebra of Circulant matrices, associated with Periodic BCs, while it is necessary to get the algebra of Reflective and Anti-Reflective matrices. The symmetry property allows in all these three cases to have also a fast transform that can be employed for computing matrix–vectors products in an efficient way. In particular, we have Discrete Fourier Transform (DFT) for Circulant matrices, Discrete Cosine Transform of type III (DCT-III) for Reflective matrices [20] and Anti-Reflective Transform (ART) – strongly linked to Discrete Sine Transform of type I (DST-I) – for Anti-Reflective matrices [21].

Unfortunately, this is not the case for Toeplitz matrices, associated with Zero BCs, i.e. $W^{\mathcal{Z}} = T$, where

$$T = \begin{pmatrix}
w_0 & w_1 & w_2 & \dots & w_\ell & & & & & \\
w_1 & w_0 & w_1 & w_2 & \ddots & w_\ell & & & & \\
w_2 & w_1 & w_0 & w_1 & w_2 & \ddots & w_\ell & & & \\
\vdots & w_2 & w_1 & w_0 & w_1 & w_2 & \ddots & \ddots & & \\
w_\ell & \ddots & w_2 & w_1 & \ddots & \ddots & \ddots & \ddots & w_\ell & \\
 & w_\ell & \ddots & w_2 & \ddots & \ddots & w_1 & w_2 & \ddots & w_\ell \\
 & & w_\ell & \ddots & \ddots & w_1 & w_0 & w_1 & w_2 & \vdots \\
 & & & \ddots & \ddots & w_2 & w_1 & w_0 & w_1 & w_2 \\
 & & & & w_\ell & \ddots & w_2 & w_1 & w_0 & w_1 \\
 & & & & & w_\ell & \dots & w_2 & w_1 & w_0
\end{pmatrix}_{n\times n}. \tag{12}$$

In case of Periodic BCs, we have Circulant matrices that have this form

$$W^{\mathcal{P}} = \begin{pmatrix}
w_0 & w_1 & \dots & w_\ell & & & & w_\ell & \dots & w_1 \\
w_1 & w_0 & w_1 & \ddots & w_\ell & & & & \ddots & \vdots \\
\vdots & w_1 & w_0 & w_1 & \ddots & w_\ell & & & & w_\ell \\
w_\ell & \ddots & w_1 & w_0 & w_1 & \ddots & \ddots & & & \\
 & w_\ell & \ddots & w_1 & w_0 & \ddots & \ddots & w_\ell & & \\
 & & w_\ell & \ddots & \ddots & \ddots & w_1 & \ddots & w_\ell & \\
 & & & \ddots & \ddots & w_1 & w_0 & w_1 & \ddots & w_\ell \\
w_\ell & & & & w_\ell & \ddots & w_1 & w_0 & w_1 & \vdots \\
\vdots & \ddots & & & & w_\ell & \ddots & w_1 & w_0 & w_1 \\
w_1 & \dots & w_\ell & & & & w_\ell & \dots & w_1 & w_0
\end{pmatrix}_{n\times n}. \tag{13}$$

Please cite this article as: A. Cicone and P. Dell'Acqua, Study of boundary conditions in the Iterative Filtering method for the decomposition of nonstationary signals, Journal of Computational and Applied Mathematics (2019), https://doi.org/10.1016/j.cam.2019.04.028.

If we denote by i the imaginary unit, $W^{\mathcal{P}}$ can be diagonalized by $Q^{\mathcal{P}}$, defined as

$$[Q^{\mathcal{P}}]_{i,j} = [\sqrt{n}F^{-1}]_{i,j} = \frac{1}{\sqrt{n}} e^{\frac{2(i-1)(j-1)\pi \mathrm{i}}{n}}, \qquad i,j = 1,\dots,n, \tag{14}$$

where F is the n-dimensional DFT. Eigenvalues of $W^{\mathcal{P}}$ can be computed by the formula

$$\lambda_i^{\mathcal{P}} = w_0 + 2\sum_{j=1}^{\ell} w_j \cos\left(\frac{2j(i-1)\pi}{n}\right) \qquad \text{for } i = 1,\dots,n \tag{15}$$

In the Reflective case, we have $W^{\mathcal{R}} = T + H^{\mathcal{R}}$, where $H^{\mathcal{R}}$ is a Hankel matrix

$$H^{\mathcal{R}} = \begin{pmatrix} w_1 & w_2 & w_3 & \dots & w_\ell & & & & & \\ w_2 & w_3 & \iddots & \iddots & & & & & & \\ w_3 & \iddots & \iddots & & & & & & & \\ \vdots & \iddots & & & & & & & & \\ w_\ell & & & & & & & & & w_\ell \\ & & & & & & & & \iddots & \vdots \\ & & & & & & & \iddots & \iddots & w_3 \\ & & & & & & \iddots & \iddots & w_3 & w_2 \\ & & & & & w_\ell & \dots & w_3 & w_2 & w_1 \end{pmatrix}_{n\times n}. \tag{16}$$

$W^{\mathcal{R}}$ can be diagonalized by $Q^{\mathcal{R}}$, that is the n-dimensional DCT-III, having entries

$$[Q^{\mathcal{R}}]_{i,j} = \sqrt{\frac{2-\delta_{i1}}{n}} \cos\left(\frac{(i-1)(2j-1)\pi}{2n}\right), \qquad i,j = 1,\dots,n, \tag{17}$$

where δ_{ij} denotes the Kronecker delta. Eigenvalues of $W^{\mathcal{R}}$ can be obtained by the formula

$$\lambda_i^{\mathcal{R}} = \frac{[Q^{\mathcal{R}}(W^{\mathcal{R}}\mathbf{e}_1)]_i}{[Q^{\mathcal{R}}\mathbf{e}_1]_i}, \tag{18}$$

where $\mathbf{e}_1 = (1,0,\dots,0)^T \in \mathbb{R}^n$. Therefore, using the variable $t = \frac{(i-1)\pi}{2n}$, and exploiting

$$\cos(2jt \mp t) = \cos(2jt)\cos(t) \pm \sin(2jt)\sin(t)$$

we get that in the Reflective case the eigenvalues can be computed, for $i = 1,\dots,n$, as

$$\begin{aligned} \lambda_i^{\mathcal{R}} &= \sum_{j=1}^{n} [W^{\mathcal{R}}]_{1,j} \frac{\cos\left((2j-1)\frac{(i-1)\pi}{2n}\right)}{\cos\left(\frac{(i-1)\pi}{2n}\right)} \\ &= w_0 + \sum_{j=1}^{\ell} w_j \frac{\cos((2j-1)t) + \cos((2j+1)t)}{\cos(t)} \\ &= w_0 + 2\sum_{j=1}^{\ell} w_j \cos(2jt) \\ &= w_0 + 2\sum_{j=1}^{\ell} w_j \cos\left(\frac{j(i-1)\pi}{n}\right) \end{aligned} \tag{19}$$

In the Anti-Reflective case, the structure of the matrix is more involved, namely

$$W^{\mathcal{AR}} = \begin{pmatrix} z_1 + w_0 & 0 & \dots & \dots & \dots & 0 & 0 \\ z_2 + w_1 & & & & & & \vdots \\ \vdots & & & & & & \vdots \\ z_\ell + w_{\ell-1} & & & & & & 0 \\ w_\ell & & & \hat{W}^{\mathcal{AR}} & & & w_\ell \\ 0 & & & & & & z_\ell + w_{\ell-1} \\ \vdots & & & & & & \vdots \\ \vdots & & & & & & z_2 + w_1 \\ 0 & 0 & \dots & \dots & \dots & 0 & z_1 + w_0 \end{pmatrix}_{n\times n}, \tag{20}$$

where $z_j = 2\sum_{k=j}^{\ell} w_k$ and $\hat{W}^{\mathcal{AR}} = PW^{\mathcal{AR}}P^T$, with

$$P = \begin{pmatrix} 0 & 1 & & & & 0 \\ 0 & & 1 & & & 0 \\ \vdots & & & \ddots & & \vdots \\ 0 & & & & 1 & 0 \\ 0 & & & & & 1 & 0 \end{pmatrix}_{(n-2)\times n}. \tag{21}$$

Moreover, $\hat{W}^{\mathcal{AR}} = \hat{T} - \hat{H}^{\mathcal{AR}}$, where $\hat{T}$ is a Toeplitz matrix

$$\hat{T} = \begin{pmatrix} w_0 & w_1 & \dots & w_\ell & & & & \\ w_1 & w_0 & w_1 & \ddots & w_\ell & & & \\ \vdots & w_1 & w_0 & w_1 & \ddots & \ddots & & \\ w_\ell & \ddots & w_1 & w_0 & \ddots & \ddots & w_\ell & \\ & w_\ell & \ddots & \ddots & \ddots & w_1 & \ddots & w_\ell \\ & & \ddots & \ddots & w_1 & w_0 & w_1 & \vdots \\ & & & w_\ell & \ddots & w_1 & w_0 & w_1 \\ & & & & w_\ell & \dots & w_1 & w_0 \end{pmatrix}_{(n-2)\times(n-2)}, \tag{22}$$

while $\hat{H}^{\mathcal{AR}}$ is a Hankel matrix

$$\hat{H}^{\mathcal{AR}} = \begin{pmatrix} w_2 & w_3 & \dots & w_\ell & & & & \\ w_3 & \iddots & \iddots & & & & & \\ \vdots & \iddots & & & & & & \\ w_\ell & & & & & & & w_\ell \\ & & & & & & \iddots & \vdots \\ & & & & & \iddots & \iddots & w_3 \\ & & & & w_\ell & \dots & w_3 & w_2 \end{pmatrix}_{(n-2)\times(n-2)}. \tag{23}$$

$\hat{W}^{\mathcal{AR}}$ can be diagonalized by $\hat{Q}^{\mathcal{AR}}$, that is the $(n-2)$-dimensional DST-I, having entries

$$[\hat{Q}^{\mathcal{AR}}]_{i,j} = \sqrt{\frac{2}{n-1}} \sin\left(\frac{ij\pi}{n-1}\right), \qquad i,j = 1,\dots,n-2. \tag{24}$$

Eigenvalues of $\hat{W}^{\mathcal{AR}}$ can be obtained as

$$\hat{\lambda}_i^{\mathcal{AR}} = \frac{[\hat{Q}^{\mathcal{AR}}(\hat{W}^{\mathcal{AR}}\hat{\mathbf{e}}_1)]_i}{[\hat{Q}^{\mathcal{AR}}\hat{\mathbf{e}}_1]_i} \tag{25}$$

Please cite this article as: A. Cicone and P. Dell'Acqua, Study of boundary conditions in the Iterative Filtering method for the decomposition of nonstationary signals, Journal of Computational and Applied Mathematics (2019), https://doi.org/10.1016/j.cam.2019.04.028.

where $\hat{\mathbf{e}}_1 = (1, 0, \dots, 0)^T \in \mathbb{R}^{n-2}$. Therefore, using the variable $t = \frac{i\pi}{n-1}$, and exploiting the following formulas

$$\begin{aligned}
\sin(2t) &= 2\sin(t)\cos(t)\\
\cos(2t) &= 1 - 2\sin^2(t)\\
\sin((j+2)t) - \sin(jt) &= \sin(jt)\cos(2t) + \sin(2t)\cos(jt) - \sin(jt)\\
&= \sin(jt)(1 - 2\sin^2(t)) + 2\sin(t)\cos(t)\cos(jt) - \sin(jt)\\
&= -2\sin(jt)\sin^2(t) + 2\sin(t)\cos(t)\cos(jt)\\
2\sin(jt)\sin(t) &= \cos(jt - t) - \cos(jt + t)\\
2\cos(t)\cos(jt) &= \cos(jt - t) - \cos(jt + t)
\end{aligned}$$

we get that the eigenvalues of $\hat{W}^{\mathcal{AR}}$ can be computed, for $i = 1, \dots, n-2$, as

$$\begin{aligned}
\hat{\lambda}_i^{\mathcal{AR}} &= \sum_{j=1}^{n-2} [\hat{W}^{\mathcal{AR}}]_{1,j} \frac{\sin\left(\frac{ji\pi}{n-1}\right)}{\sin\left(\frac{i\pi}{n-1}\right)}\\
&= w_0 + w_1 \frac{\sin(2t)}{\sin(t)} + \sum_{j=1}^{\ell-1} w_{j+1} \frac{\sin((j+2)t)}{\sin(t)} - w_{j+1}\frac{\sin(jt)}{\sin(t)}\\
&= w_0 + 2w_1\cos(t) + \sum_{j=1}^{\ell-1} w_{j+1}\,(2\cos(t)\cos(jt) - 2\sin(jt)\sin(t))\\
&= w_0 + 2w_1\cos(t) + 2\sum_{j=1}^{\ell-1} w_{j+1}\cos((j+1)t)\\
&= w_0 + 2w_1\cos(t) + 2\sum_{j=2}^{\ell} w_j \cos(jt)\\
&= w_0 + 2\sum_{j=1}^{\ell} w_j \cos\left(\frac{ji\pi}{n-1}\right)
\end{aligned} \tag{26}$$

By Lemma 3.1 in [21], we know that the eigenvalues of $W^{\mathcal{AR}}$ are given by 1, with multiplicity two, and the eigenvalues $\{\hat{\lambda}_i^{\mathcal{AR}}\}_{i=1,\dots,n-2}$ of $\hat{W}^{\mathcal{AR}}$.

Looking at the structure of the matrices presented, it can be easily verified that the eigenvector $u_1^{\mathcal{P}}$ associated with $\lambda_1^{\mathcal{P}} = 1$ is $(1, \dots, 1)^T$, the eigenvector $u_1^{\mathcal{R}}$ associated with $\lambda_1^{\mathcal{R}} = 1$ is $(1, \dots, 1)^T$, and the eigenvectors associated with $\lambda_1^{\mathcal{AR}} = \lambda_2^{\mathcal{AR}} = 1$ are $u_1^{\mathcal{AR}} = (0, 1, 2, \dots, n-2, n-1)^T$ and $u_2^{\mathcal{AR}} = (n-1, n-2, \dots, 2, 1, 0)^T$, respectively.

We notice that $Q^{\mathcal{P}}$, $Q^{\mathcal{R}}$ and $\hat{Q}^{\mathcal{AR}}$ are all unitary matrices. However, the last one is linked to $\hat{W}^{\mathcal{AR}}$, so we also need to know how to diagonalize the original matrix $W^{\mathcal{AR}}$. In other words, based on DST-I, we need to introduce ART. Unfortunately this transform is not unitary, since the matrices in Anti-Reflective algebra are in general not normal. Recalling theoretical results reported in [13,22,23], we have that $W^{\mathcal{AR}}$ can be diagonalized by $Q^{\mathcal{AR}}$, that is the n-dimensional ART, defined as follows

$$Q^{\mathcal{AR}} = \begin{pmatrix}
(n-1)\eta^{-1} & 0 & \dots & \dots & \dots & 0 & 0\\
(n-2)\eta^{-1} & & & & & & \eta^{-1}\\
(n-3)\eta^{-1} & & & & & & 2\eta^{-1}\\
\vdots & & & & & & \vdots\\
\vdots & & & \hat{Q}^{\mathcal{AR}} & & & \vdots\\
\vdots & & & & & & \vdots\\
2\eta^{-1} & & & & & & (n-3)\eta^{-1}\\
\eta^{-1} & & & & & & (n-2)\eta^{-1}\\
0 & 0 & \dots & \dots & \dots & 0 & (n-1)\eta^{-1}
\end{pmatrix}_{n\times n}, \tag{27}$$

where the parameter $\eta = \sqrt{\sum_{j=0}^{n-1} j^2}$ is introduced to normalize the first and the last column, which come from the eigenvectors $u_1^{\mathcal{AR}}$ and $u_2^{\mathcal{AR}}$.

In summary, in this Section we have introduced several BCs alternative to periodic ones, provided descriptions of the associated structured matrices, analyzed their properties, derived formulas for the computation of their eigenvalues and

provided diagonalization formulas associated with the discrete transforms. All these results will be put into play in the next section in which we investigate the convergence properties of the DIF method.

4. Spectral properties and convergence results

In this section we consider Periodic, Reflective and Anti-Reflective BCs and, exploiting results presented in Section 3, we derive spectral properties of $W^{\mathcal{BC}}$ and convergence results for the DIF algorithm.

Lemma 1. *Let $W^{\mathcal{BC}} \in \mathbb{R}^{n\times n}$ be a structured matrix constructed from a symmetric decreasing filter $\mathbf{w}$ of length $0 < \ell \leq \lfloor \frac{n-1}{2} \rfloor$, imposing Periodic, Reflective or Anti-Reflective BCs. Then $\sigma(W^{\mathcal{BC}}) \subseteq [-1, 1]$.*

Proof. By definition $W^{\mathcal{BC}}$ is a symmetric matrix, so it has a real spectrum. By considering the following estimate relative to the spectral radius

$$\rho(W^{\mathcal{BC}}) \leq \left\|W^{\mathcal{BC}}\right\|_\infty = \max_i \sum_{j=1}^{n} \left|[W^{\mathcal{BC}}]_{i,j}\right| = w_0 + 2\sum_{k=1}^{\ell} w_k = 1,$$

we can conclude that all eigenvalues lie in the interval $[-1, 1]$. □

Theorem 1. *Let $\mathbf{s} \in \mathbb{R}^n$ be the signal we want to decompose. Let $\mathbf{v}$ be a symmetric decreasing filter of length $0 < \ell' \leq \lfloor \frac{n-1}{4} \rfloor$ and $\mathbf{w} = \mathbf{v} * \mathbf{v}$ be a symmetric decreasing filter of length $0 < \ell \leq \lfloor \frac{n-1}{2} \rfloor$ derived as the convolution of $\mathbf{v}$ with itself. Then for the matrix $W^{\mathcal{BC}} \in \mathbb{R}^{n\times n}$ constructed from $\mathbf{w}$ and Periodic, Reflective or Anti-Reflective BCs, it holds that $\sigma(W^{\mathcal{BC}}) \subseteq [0, 1]$. Moreover, $\lambda_1^{\mathcal{P}} = 1$ and $\{\lambda_i^{\mathcal{P}}\}_{i=2,\dots,n} \subseteq [0, 1)$, $\lambda_1^{\mathcal{R}} = 1$ and $\{\lambda_i^{\mathcal{R}}\}_{i=2,\dots,n} \subseteq [0, 1)$, $\lambda_1^{\mathcal{AR}} = \lambda_2^{\mathcal{AR}} = 1$ and $\{\lambda_i^{\mathcal{AR}}\}_{i=3,\dots,n} \subseteq [0, 1)$.*

Proof. As already said, in case of Periodic, Reflective or Anti-Reflective BCs we are in a matrix algebra; this means that the matrix product gives rise to a matrix which can still be interpreted as a matrix constructed from a filter and the same BCs. In particular, thanks to the fact that $\ell' \leq \lfloor \frac{n-1}{4} \rfloor$, such filter can be computed by means of a convolution. Thus, if we denote by $V^{\mathcal{BC}}$ the structured matrix associated with the filter $\mathbf{v}$, we have that $W^{\mathcal{BC}} = (V^{\mathcal{BC}})^2$. By Lemma 1, $\sigma(V^{\mathcal{BC}}) \subseteq [-1, 1]$, therefore $\sigma(W^{\mathcal{BC}}) \subseteq [0, 1]$.

Moreover, in case of Periodic BCs, if we consider (15) with $i = 1$, we get $\lambda_1^{\mathcal{P}} = 1$, while for $1 < i \leq n$ we have a convex combination of cosine values (each of them strictly less than 1), except for the first term multiplied by w_0 which is equal to 1. Clearly this sum cannot equal to 1, so it has a value $0 \leq \lambda_i^{\mathcal{P}} < 1, \forall i = 2, \dots, n$.

In case of Reflective BCs, if we consider (19) with $i = 1$, we get $\lambda_1^{\mathcal{R}} = 1$, while for $1 < i \leq n$ we have a convex combination of cosine values (each of them strictly less than 1), except for the first term multiplied by w_0 which is equal to 1. Clearly this sum cannot equal to 1, so it has a value $0 \leq \lambda_i^{\mathcal{R}} < 1, \forall i = 2, \dots, n$.

In case of Anti-Reflective BCs, if we consider (26) for $i = 1, \dots, n-2$ we have a convex combination of cosine values (each of them strictly less than 1), except for the first term multiplied by w_0 which is equal to 1. Clearly this sum cannot equal to 1, so it has a value $0 \leq \lambda_i^{\mathcal{AR}} < 1, \forall i = 3, \dots, n$. Therefore $n-2$ eigenvalues of $W^{\mathcal{BC}}$ belong to the interval $[0, 1)$, while the remaining two are equal to 1. □

In the following Lemma we summarize diagonalization results presented in Section 3.

Lemma 2. *Let $W^{\mathcal{BC}} \in \mathbb{R}^{n\times n}$ be a matrix constructed from a symmetric filter $\mathbf{w}$ and Periodic, Reflective or Anti-Reflective BCs. Then*

$$W^{\mathcal{BC}} = Q^{\mathcal{BC}} D^{\mathcal{BC}} (Q^{\mathcal{BC}})^{-1}, \tag{28}$$

i.e. $W^{\mathcal{BC}}$ can be diagonalized by $Q^{\mathcal{BC}}$, whose columns are eigenvectors of $W^{\mathcal{BC}}$.

Now we are ready to discuss the convergence of DIF algorithm. The method in the limit produces IMFs that are projections of the given signal $\mathbf{s}$ onto the eigenspace of $W^{\mathcal{BC}}$ corresponding to the zero eigenvalue which has algebraic and geometric multiplicity $\zeta \in \{0, 1, \dots, n-1\}$. Clearly, if $W^{\mathcal{BC}}$ has only a trivial kernel then the method converges to the zero vector. On the other hand, if we enforce a stopping criterion, the techniques gets approximated IMFs after finitely many steps. Theorem 2 generalizes theoretical results provided in [6] for the case of Periodic BCs.

Theorem 2. *Let $\mathbf{s} \in \mathbb{R}^n$ be the signal we want to decompose. Let $\mathbf{v}$ be a symmetric decreasing filter of length $0 < \ell' \leq \lfloor \frac{n-1}{4} \rfloor$ and $\mathbf{w} = \mathbf{v} * \mathbf{v}$ a derived symmetric decreasing filter of length $0 < \ell \leq \lfloor \frac{n-1}{2} \rfloor$ given as convolution of $\mathbf{v}$ with itself. Let $W^{\mathcal{BC}} \in \mathbb{R}^{n\times n}$ be the matrix constructed from $\mathbf{w}$ and Periodic, Reflective or Anti-Reflective BCs, which can be diagonalized by $Q^{\mathcal{BC}}$, and $\zeta \in \{0, 1, \dots, n-1\}$ be the number of its zero eigenvalues. Let $\alpha^{\mathcal{BC}}$ and $\beta^{\mathcal{BC}}$ be two constants depending on the BCs at hand ($\alpha^{\mathcal{P}} = \alpha^{\mathcal{R}} = 1$, $\alpha^{\mathcal{AR}} = 3$ and $\beta^{\mathcal{P}} = \beta^{\mathcal{R}} = 1$, $\beta^{\mathcal{AR}} = 2$).*

Then, at step k of the inner loop in the DIF method, the first IMF is given by

$$\mathbf{f}_1 = Q^{\mathcal{BC}} (Z^{\mathcal{BC}})^k (Q^{\mathcal{BC}})^{-1} \mathbf{s},$$

where $Z^{\mathcal{BC}} = I - D^{\mathcal{BC}}$ *can be rewritten as*

$$Z^{\mathcal{BC}} = P \begin{pmatrix} 1-\lambda_1^{\mathcal{BC}} & & & & & & \\ & 1-\lambda_2^{\mathcal{BC}} & & & & & \\ & & \ddots & & & & \\ & & & 1-\lambda_{n-\zeta}^{\mathcal{BC}} & & & \\ & & & & 1 & & \\ & & & & & \ddots & \\ & & & & & & 1 \end{pmatrix} P^T$$

by means of a suitable permutation matrix P*, and the first* $\beta^{\mathcal{BC}}$ *elements that appear on the diagonal are equal to zero. Letting* k *to go to infinity, the first outer loop step of the DIF method converges to*

$$\mathbf{f}_1 = Q^{\mathcal{BC}} Z_\infty (Q^{\mathcal{BC}})^{-1}\mathbf{s},$$

where Z_∞ *is a diagonal matrix whose entries are all zero, except* ζ *diagonal elements equal to one.*

Moreover, fixed $\delta > 0$*, for the minimum* $k_0 \in \mathbb{N}$ *such that it holds true the inequality*

$$\frac{k_0^{k_0}}{(k_0+1)^{k_0+1}} < \frac{\delta}{\alpha^{\mathcal{BC}} \|(Q^{\mathcal{BC}})^{-1}\mathbf{s}\|_\infty \sqrt{n-\beta^{\mathcal{BC}}-\zeta}},$$

we have that the following stopping criterion is satisfied

$$\left\|\mathbf{s}_{k+1}^1 - \mathbf{s}_k^1\right\|_2 < \delta, \qquad \forall k \geq k_0,$$

so the DIF algorithm takes finitely many steps to produce the first IMF.

Proof. The first part of the theorem follows from the definition of DIF method in matrix form and from Lemma 2. In fact, at step k of the inner loop in the DIF method, the first IMF is given by

$$\mathbf{f}_1 = (I - W^{\mathcal{BC}})^k \mathbf{s} = Q^{\mathcal{BC}} (Z^{\mathcal{BC}})^k (Q^{\mathcal{BC}})^{-1}\mathbf{s},$$

Moreover, by Theorem 1 we know that $W^{\mathcal{BC}}$ has $\beta^{\mathcal{BC}}$ eigenvalues equal to 1. On the other hand, letting k go to infinity, we get

$$\mathbf{f}_1 = \lim_{k\to\infty} Q^{\mathcal{BC}} (Z^{\mathcal{BC}})^k (Q^{\mathcal{BC}})^{-1}\mathbf{s} = Q^{\mathcal{BC}} Z_\infty (Q^{\mathcal{BC}})^{-1}\mathbf{s}.$$

The second part of the theorem follows from

$$\begin{aligned}
\|\mathbf{s}_{k+1}^1 - \mathbf{s}_k^1\|_2 &= \|(I - W^{\mathcal{BC}})^{k+1}\mathbf{s} - (I - W^{\mathcal{BC}})^k \mathbf{s}\|_2 \\
&= \|Q^{\mathcal{BC}}(I - D^{\mathcal{BC}})^{k+1}(Q^{\mathcal{BC}})^{-1}\mathbf{s} - Q^{\mathcal{BC}}(I - D^{\mathcal{BC}})^k (Q^{\mathcal{BC}})^{-1}\mathbf{s}\|_2 \\
&= \|Q^{\mathcal{BC}}(Z^{\mathcal{BC}})^k ((I - D^{\mathcal{BC}}) - I)(Q^{\mathcal{BC}})^{-1}\mathbf{s}\|_2 \\
&= \|Q^{\mathcal{BC}}(Z^{\mathcal{BC}})^k D^{\mathcal{BC}} (Q^{\mathcal{BC}})^{-1}\mathbf{s}\|_2 \\
&\leq \alpha^{\mathcal{BC}} \|(Z^{\mathcal{BC}})^k D^{\mathcal{BC}} (Q^{\mathcal{BC}})^{-1}\mathbf{s}\|_2 \\
&\leq \alpha^{\mathcal{BC}} \left\| P \begin{pmatrix} (1-\lambda_1^{\mathcal{BC}})^k \lambda_1^{\mathcal{BC}} & & & & \\ & \ddots & & & \\ & & (1-\lambda_{n-\zeta}^{\mathcal{BC}})^k \lambda_{n-\zeta}^{\mathcal{BC}} & & \\ & & & 0 & \\ & & & & \ddots \\ & & & & & 0 \end{pmatrix} P^T \begin{pmatrix} \|(Q^{\mathcal{BC}})^{-1}\mathbf{s}\|_\infty \\ \vdots \\ \|(Q^{\mathcal{BC}})^{-1}\mathbf{s}\|_\infty \end{pmatrix} \right\|_2 \\
&\leq \alpha^{\mathcal{BC}} \sqrt{n-\beta^{\mathcal{BC}}-\zeta} \left(1 - \frac{1}{k+1}\right)^k \frac{1}{k+1} \|(Q^{\mathcal{BC}})^{-1}\mathbf{s}\|_\infty
\end{aligned}$$

where P is a suitable permutation matrix and $\alpha^{\mathcal{BC}}$ depends on the value of $\|Q^{\mathcal{BC}}\|_2$. So it is equal to 1 for Periodic and Reflective BCs, since $Q^{\mathcal{P}}$ and $Q^{\mathcal{R}}$ are unitary matrices, while in the Anti-Reflective case it is equal to 3 because we can rewrite $Q^{\mathcal{AR}}$ in (27) as the sum of three matrices, having non-zero elements only in the first column, in the last column and in the central part corresponding to $\hat{Q}^{\mathcal{AR}}$, which is unitary. Then we can apply the triangle inequality, exploiting also the fact that the Euclidean norm of each splitting matrix is equal to 1. To derive the last inequality, we use the fact that the function $(1-\lambda)^k\lambda$ achieves its maximum at $\lambda = \frac{1}{k+1}$ for $\lambda \in [0,\ 1]$. Hence the stopping criterion is fulfilled for k_0 minimum natural number such that $k_0^{k_0}/(k_0+1)^{k_0+1} < \delta/\alpha^{\mathcal{BC}} \|(Q^{\mathcal{BC}})^{-1}\mathbf{s}\|_\infty \sqrt{n-\beta^{\mathcal{BC}}-\zeta}$. □

Please cite this article as: A. Cicone and P. Dell'Acqua, Study of boundary conditions in the Iterative Filtering method for the decomposition of nonstationary signals, Journal of Computational and Applied Mathematics (2019), https://doi.org/10.1016/j.cam.2019.04.028.

The DIF algorithm described and studied so far requires to reimpose the BCs at every iteration of the inner loop. In order to reduce the errors and their propagation, the idea is to impose the BCs only in the first step of each inner loop, or even better only in the beginning of the outer loop, and then let the solution to evolve freely. This is the rationale behind the extended approach described in the next section.

5. Extended iterative filtering

Given the matrix

$$R = \left(O_{n\times p}\ I_{n\times n}\ O_{n\times p} \right)_{n\times(n+2p)}, \tag{29}$$

where O is matrix of all zeros and I is the identity matrix, we can define the Extended Iterative Filtering (EIF) algorithm, whose pseudocode is given in Algorithm 2. The main idea is to first extend as we like the given signal s of p entries per side outside the boundaries and then apply a periodic version of the DIF algorithm to the extended signal $\mathbf{s}^{\mathcal{BC}} \in \mathbb{R}^{(n+2p)}$. Therefore the EIF method is always associated with a Circulant matrix $\ddot{W}_m^{\mathcal{P}} \in \mathbb{R}^{(n+2p)\times(n+2p)}$, whose structure does not depend on the BCs, and the signal $\mathbf{s}^{\mathcal{BC}} \in \mathbb{R}^{(n+2p)}$ extended of $2p$ by means of any BCs. In particular in this framework the BCs do not have to be limited, as in the previous section, to the ones that induce a special matrix structure in $\ddot{W}_m^{\mathcal{BC}}$. Hence we are completely free to extend the original signal outside the boundaries as we like. Moreover, we notice that in Algorithm 2 there is only one step involving the use of BCs, whereas in Algorithm 1 the BCs are imposed at every step of the Inner Loop. In doing so we reduce the impact of the errors introduced in the decomposition by the extension of the signal outside the boundaries. Furthermore, we remark that employing Periodic BCs allows to reduce the computational burden of IF. In fact the algorithm can be rewritten using Fast Fourier Transform (FFT) to become what is known as Fast Iterative Filtering (FIF) [6].

Algorithm 2 Extended Iterative Filtering IMFs = EIF(s, h)

$\mathbf{s}^{\mathcal{BC}}(x_i) = \mathbf{s}(x_i)$, $i = 0, \dots, n-1$
apply BCs to compute $\mathbf{s}^{\mathcal{BC}}(x_i)$, $i = -p, \dots, -1$ and $i = n, \dots, n-1+p$
$m = 1$
$\mathbf{s}_1^m = \mathbf{s}^{\mathcal{BC}}$
while the number of extrema of $\mathbf{s}_1^m \geq 2$ **do**
  $k = 1$
  compute the filter length ℓ_m for the signal $\mathbf{s}_k^m$
  compute $\mathbf{w}_m$ (having h and ℓ_m)
  while the stopping criterion is not satisfied **do**
    $\mathbf{s}_{k+1}^m = (I - \ddot{W}_m^{\mathcal{P}})\mathbf{s}_k^m$
    $k = k + 1$
  end while
  $\mathbf{f}_m = \mathbf{s}_k^m$
  $\mathbf{s}_1^{m+1} = \mathbf{s}_1^m - \mathbf{f}_m$
  $m = m + 1$
end while
$\mathbf{f}_m = \mathbf{s}_1^m$
IMFs = $\{R\mathbf{f}_1, \dots, R\mathbf{f}_m\}$

The algorithm written in this way allows to derive an a priori estimate of how much the error introduced by the extensions at the boundaries diffuses inside the computed IMFs in the iterations.

We start by denoting as $\mathbf{f}_1 \in \mathbb{R}^n$ the first approximated IMF computed by the EIF algorithm. $\bar{\mathbf{f}}_1 \in \mathbb{R}^n$ represents the first exact IMF, whereas $\mathbf{s}^{\mathcal{BC}} \in \mathbb{R}^{n+2p}$ the signal extended according to some a priori chosen BCs and $\ddot{\mathbf{s}} \in \mathbb{R}^{n+2p}$ the unknown real signal extended also outside the boundaries. Then we can split these last two vectors considering the portion of signal inside and outside the field of view identified by the boundaries, and get

$$\mathbf{s}^{\mathcal{BC}} = \mathbf{s}_{\text{in}}^{\mathcal{BC}} + \mathbf{s}_{\text{out}}^{\mathcal{BC}} \tag{30}$$

and

$$\ddot{\mathbf{s}} = \ddot{\mathbf{s}}_{\text{in}} + \ddot{\mathbf{s}}_{\text{out}}. \tag{31}$$

Clearly $\mathbf{s}_{\text{in}}^{\mathcal{BC}} = \ddot{\mathbf{s}}_{\text{in}}$.

We have that

$$\begin{aligned}\mathbf{f}_1 &= R(I - \ddot{W}_1^{\mathcal{P}})^k \mathbf{s}^{\mathcal{BC}} \\ &= R(I - \ddot{W}_1^{\mathcal{P}})^k (\mathbf{s}_{\text{in}}^{\mathcal{BC}} + \mathbf{s}_{\text{out}}^{\mathcal{BC}} + \ddot{\mathbf{s}}_{\text{out}} - \ddot{\mathbf{s}}_{\text{out}}) \\ &= R(I - \ddot{W}_1^{\mathcal{P}})^k \ddot{\mathbf{s}} + R(I - \ddot{W}_1^{\mathcal{P}})^k (\mathbf{s}_{\text{out}}^{\mathcal{BC}} - \ddot{\mathbf{s}}_{\text{out}})\end{aligned}$$

Please cite this article as: A. Cicone and P. Dell'Acqua, Study of boundary conditions in the Iterative Filtering method for the decomposition of nonstationary signals, Journal of Computational and Applied Mathematics (2019), https://doi.org/10.1016/j.cam.2019.04.028.

where the first term tends to $\bar{\mathbf{f}}_1$, while the second term it propagates itself from the boundaries inside the field of view as k increases.

In general it is not possible to estimate the difference $\mathbf{s}_{\text{out}}^{\mathcal{BC}} - \ddot{\mathbf{s}}_{\text{out}}$. However the approximation of the real signal outside the boundaries $\mathbf{s}_{\text{out}}^{\mathcal{BC}}$ produces an error $\mathbf{s}_{\text{out}}^{\mathcal{BC}} - \ddot{\mathbf{s}}_{\text{out}}$ which can always be upper bounded by a constant function whose value is given by $\chi > 0$.

We propose here to use the value $\chi = \max\left(\left|\mathbf{s}_{\text{in}}^{\mathcal{BC}}\right|\right) = \max\left(|\ddot{\mathbf{s}}_{\text{in}}|\right)$. This value provides, in many cases, a reasonable overestimation of the actual unknown value of the error.

Now the question is how the error $R(I - \ddot{W}_1^{\mathcal{P}})^k(\mathbf{s}_{\text{out}}^{\mathcal{BC}} - \ddot{\mathbf{s}}_{\text{out}})$ propagates inside the field of view during the iterations. We can estimate an upper bound for the error inside the field of view at step k of the iterations using the following formula

$$\text{err}_k = R(I - \ddot{W}_1^{\mathcal{P}})^k \mathbf{u} = R\left(I - \binom{k}{1}\ddot{W}_1^{\mathcal{P}} + \binom{k}{2}\left(\ddot{W}_1^{\mathcal{P}}\right)^2 + \cdots (-1)^k \left(\ddot{W}_1^{\mathcal{P}}\right)^k\right)\mathbf{u}, \tag{32}$$

where $\mathbf{u} \in \mathbb{R}^{n+2p}$ is a vector equal to χ outside the field of view and 0 inside.

A potential upper bound of the error for each point x_i inside the field of view can be computed as

$$\text{ub}_k(x_i) = \max_{j \le k}\left(\left|\text{err}_j(x_i)\right|\right), \tag{33}$$

where k is the number of iterations. This is just an estimate because in general the actual error value introduced by the extension of the signal outside the boundaries, that we are assuming here for simplicity to be constant and equal to $\chi = \max\left(|\ddot{\mathbf{s}}_{\text{in}}|\right)$, is unknown.

We point out here that, if we deal with artificial examples and we consider DIF algorithm employing some specific BCs, we can compute the actual error using the formula

$$\text{err}_k^{\mathcal{BC}}(x_i) = \left|\mathbf{f}_1(x_i) - \bar{\mathbf{f}}_1(x_i)\right|, \tag{34}$$

where k is the number of iterations required to produce the approximated IMF $\mathbf{f}_1$, while $\bar{\mathbf{f}}_1$ is the first exact IMF.

6. Numerical results

In order to show how DIF method performs when we employ different BCs, we present four simple artificial examples, in which the signal is generated as summation of one IMF and a trend, as well as two real life signals. In particular, we analyze how the errors introduced outside the boundaries propagate inside the field of view, evaluating the performance of formula (32) for the a priori estimation of the error when there is no knowledge on the behavior of the signal outside the boundaries.

Regarding the EIF strategy, since we obtain very similar numerical results to the DIF method, we prefer not to report them. The EIF algorithm in this work is mainly useful to derive an a priori estimate of the error coming from the extension at the boundaries. However, we point out that the EIF approach allows to employ, differently from the DIF algorithm, nonstandard BCs, as done in [16,17] for image restoration problem.

6.1. Example 1

We consider a first signal, shown on the left of Fig. 1, which can be safely extended periodically and anti-reflectively outside the boundaries. On the right of Fig. 1 we can look at decomposition obtained after 3 steps of DIF method with Reflective BCs. If we apply the DIF algorithm using Periodic, Reflective and Anti-Reflective BCs, we can extract a first IMF and measure the difference, after a fixed number of steps, between the exact IMF and the computed IMF measured in absolute value. In Fig. 2 we plot the errors introduced by each extension, as described in (34), and we compare them with the a priori estimate of the error computed using formula (33). Due to a symmetry in the signal, it is sufficient to plot the errors for the left half of the field of view. As expected, we produce a minimal error in the decomposition if we extended the signal periodically or anti-reflectively. Furthermore, the a priori upper bound estimate of the error proves to be correct.

6.2. Example 2

In this second example we consider the signal plotted in the left panel of Fig. 3, while in the right panel we show the decomposition obtained after 3 steps of DIF method with Anti-Reflective BCs. After extending the signal using Periodic, Reflective and Anti-Reflective BCs, we extract a first IMF using the DIF method. In Fig. 4 we compare the absolute values of the errors (34) introduced by the different BCs and we compute the upper bound by means of (33). Again, due to a symmetry in the curves, we report only the first half of the error plot. In this case the reflective extension works best in minimizing the error in the decomposition. Furthermore, the upper bound on the error allows to correctly estimate the error everywhere inside the field of view.

Please cite this article as: A. Cicone and P. Dell'Acqua, Study of boundary conditions in the Iterative Filtering method for the decomposition of nonstationary signals, Journal of Computational and Applied Mathematics (2019), https://doi.org/10.1016/j.cam.2019.04.028.

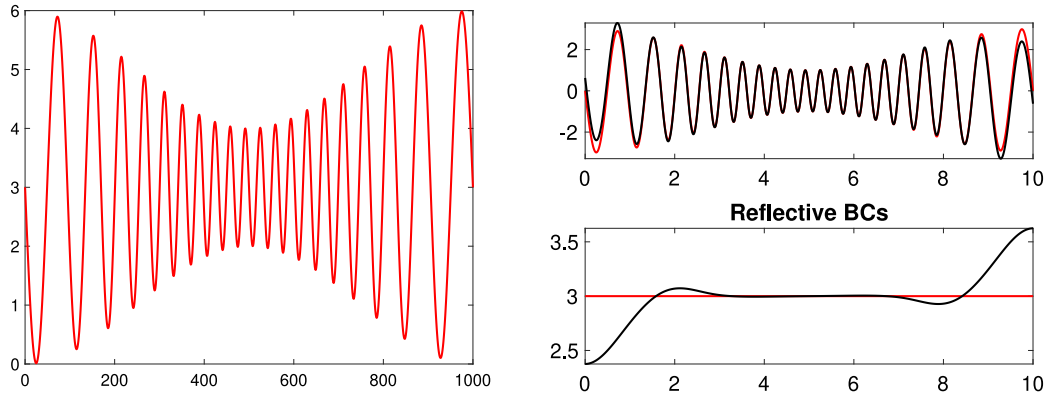

Fig. 1. Left panel: Example 1 signal. Right panel: decomposition computed by DIF method with Reflective BCs (black line) compared with the exact one (red line). (For interpretation of the references to color in this figure legend, the reader is referred to the web version of this article.)

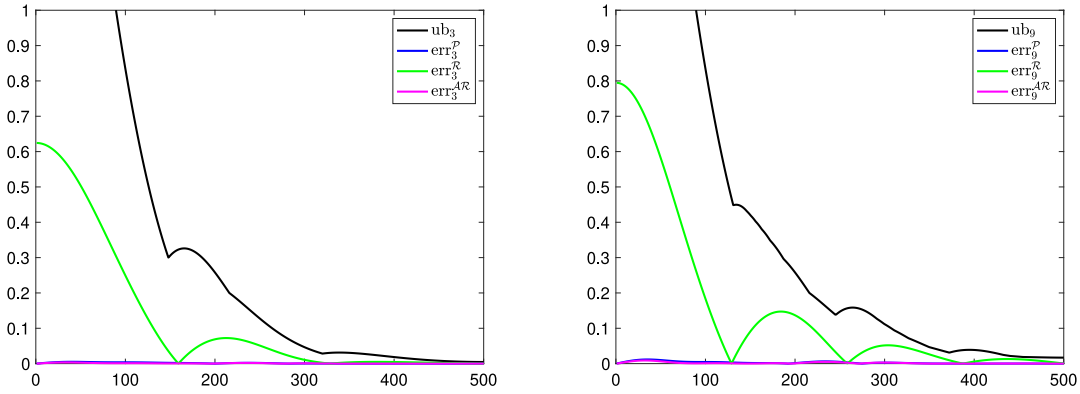

Fig. 2. Example 1 upper bound and errors measured in absolute value for Periodic, Reflective and Anti-Reflective BCs relative to 3 iterations (on the left) and 9 iterations (on the right) of DIF method.

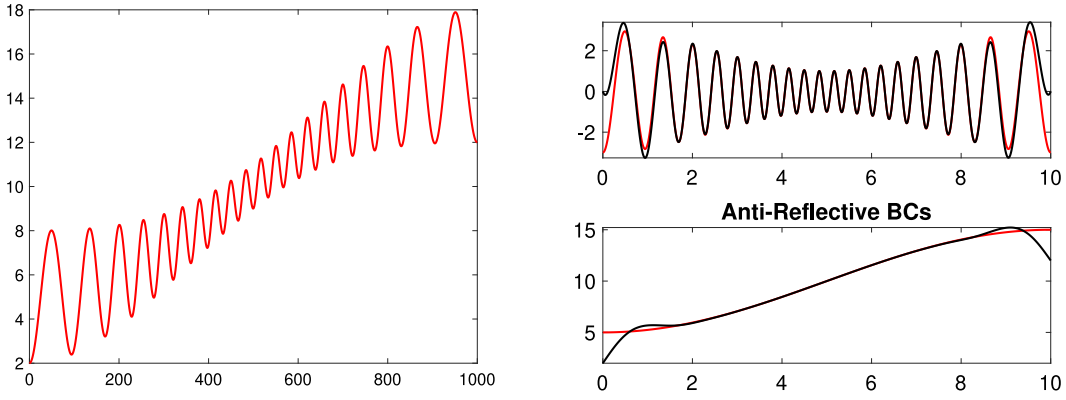

Fig. 3. Left panel: Example 2 signal. Right panel: decomposition computed by DIF method with Anti-Reflective BCs (black line) compared with the exact one (red line). (For interpretation of the references to color in this figure legend, the reader is referred to the web version of this article.)

6.3. Example 3

In this case the signal, shown in the left panel of Fig. 5, is best extended outside the boundaries using Anti-Reflective BCs. This fact is confirmed by the error curves (34) plotted in Fig. 6. Due to symmetry properties of the signal under study, we report only the first half of the error curves. Also in this example the upper bound allows to give an a priori estimate of the behavior relative to the error propagation inside the field of view.

Please cite this article as: A. Cicone and P. Dell'Acqua, Study of boundary conditions in the Iterative Filtering method for the decomposition of nonstationary signals, Journal of Computational and Applied Mathematics (2019), https://doi.org/10.1016/j.cam.2019.04.028.

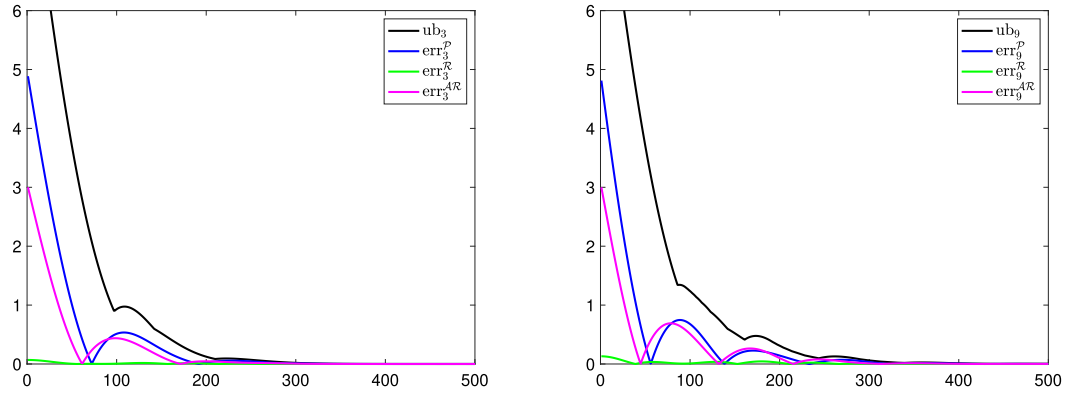

Fig. 4. Example 2 upper bound and errors measured in absolute value for Periodic, Reflective and Anti-Reflective BCs relative to 3 iterations (on the left) and 9 iterations (on the right) of DIF method.

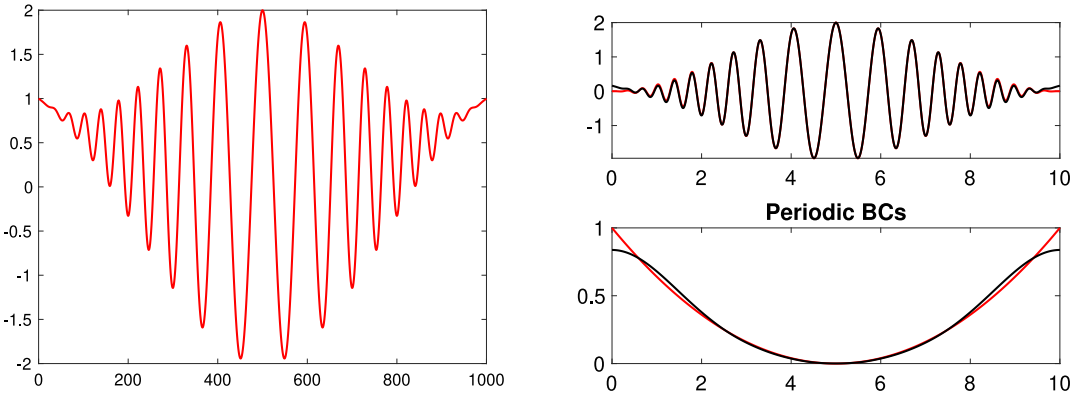

Fig. 5. Left panel: Example 3 signal. Right panel: decomposition computed by DIF method with Periodic BCs (black line) compared with the exact one (red line). (For interpretation of the references to color in this figure legend, the reader is referred to the web version of this article.)

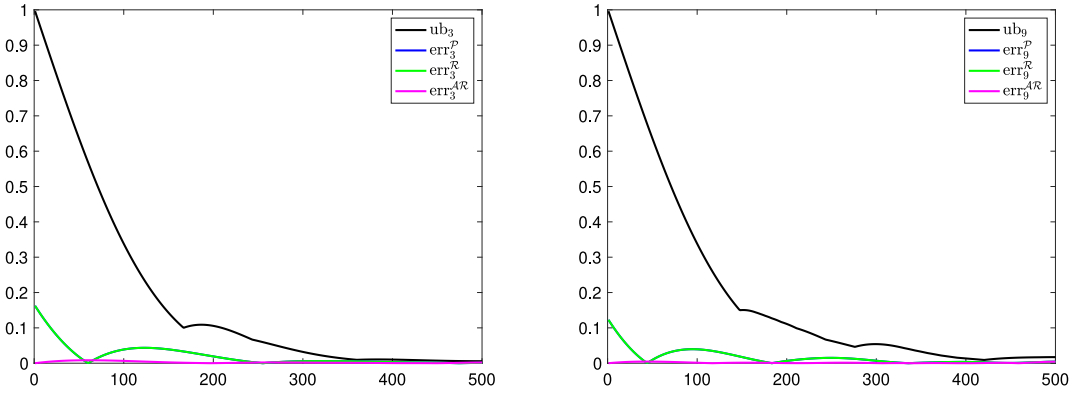

Fig. 6. Example 3 upper bound and errors measured in absolute value for Periodic, Reflective and Anti-Reflective BCs relative to 3 iterations (on the left) and 9 iterations (on the right) of DIF method.

6.4. Example 4

In this example we study how the errors induced by the extension outside the boundaries depend on the phase of the signal at the boundary. We consider a simple signal, plotted in the left panel of Fig. 7, which is a superposition of a constant trend and a plain sine. The signal support is originally given by the interval $[-333,\ 0]$ which is then extended up to 300 step by step of a $\triangle t = 0.01$. Each time we enlarge the support of a $\triangle t$ we redecompose the newly extended

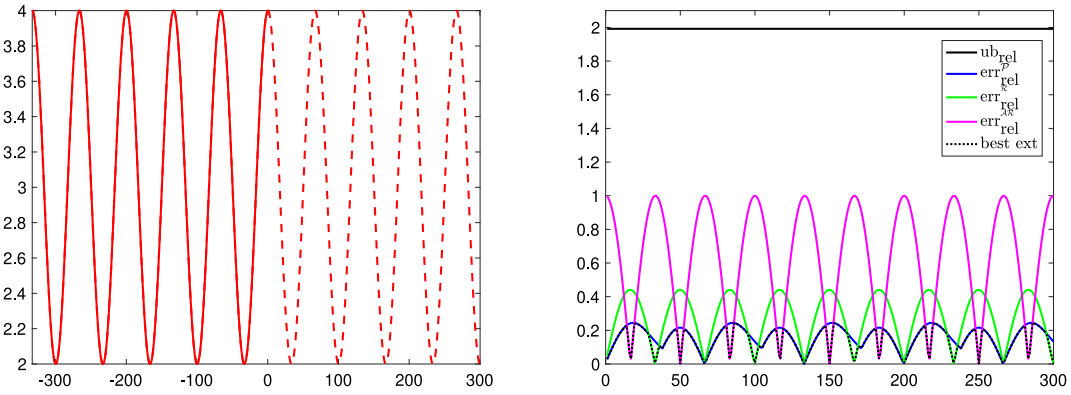

Fig. 7. Left panel: Example 4 signal. Right panel: upper bound and relative errors for different BCs and best extension.

signal using DIF with different kind of BCs. For each BCs we compute the relative error

$$\mathrm{err}_{\mathrm{rel}}^{\mathcal{BC}} = \frac{\left\|\mathbf{f}_1 - \bar{\mathbf{f}}_1\right\|_\infty}{\left\|\bar{\mathbf{f}}_1\right\|_\infty} \tag{35}$$

and the relative error upper bound

$$\mathrm{ub}_{\mathrm{rel}} = \frac{\|\mathrm{ub}_k\|_\infty}{\left\|\bar{\mathbf{f}}_1\right\|_\infty} \tag{36}$$

where $\bar{\mathbf{f}}_1$ represents the first exact IMF and ub_k is the error upper bound computed using (33) for a fixed number of iterations k. We plot the relative errors in the right panel of Fig. 7. As expected such curves have the same periodicity as the given signal. Furthermore the relative error upper bound a priori estimate proves to be valid also in this example. Finally this study allows to identify which kind of extension is performing best from a relative error point of view for each value of the phase of the signal at the boundary, dashed curve in the right panel of Fig. 7.

6.5. Example 5

The first real-world example we consider is relative to the deviation of length of the day (http://hpiers.obspm.fr/eoppc/eop/eopc04/eopc04.62-now) measured for 1000 days from 01/01/1973 to 09/28/1976. This dataset is decomposed into 5 components where 4 of them are IMFs and the last one is the trend. From the four IMFs, we can see very regular patterns: the half monthly change pattern, the monthly change pattern, the half yearly change pattern as well as the yearly change pattern.

In this case, the signal, shown in Fig. 8, is best extended outside the boundaries using Reflective BCs for some components and using Anti-Reflective BCs for other components. Since it is a real problem, the "exact" decomposition has been computed based on experimental evidences. Errors associated with DIF algorithm are due both to the use of BCs and approximate frequencies that the method tries to extract. In Fig. 9 we can find a comparison between decomposition computed by DIF method with Reflective BCs and the exact one.

6.6. Example 6

The second real-world example we consider is relative to the Earth magnetic field measured by one of the three satellites of the European Space Agency Swarm mission (http://earth.esa.int/swarm) from April 21 to 22, 2004. In particular we study the D channel of the magnetic field.

We focus on the central portion of the signal, so that we can compute the "exact" decomposition by applying DIF to the original signal, and then compare such decomposition with ones computed by DIF on the cropped signal, with the use of different BCs. As shown in the right panel of Fig. 10, in which we plot the relative error (using Euclidean norm) for DIF with different BCs, we can appreciate that Anti-Reflective ones represent the best choice in this case.

In Fig. 11 we can find decomposition computed by DIF method compared with the exact one, employing Reflective BCs and Anti-Reflective BCs. We can notice that errors are located near boundaries: Anti-Reflective BCs have a better behavior on the left border, while Reflective BCs are more accurate for the right border. This result suggests the use of different BCs on each boundary, which is possible by means of the EIF method.

Please cite this article as: A. Cicone and P. Dell'Acqua, Study of boundary conditions in the Iterative Filtering method for the decomposition of nonstationary signals, Journal of Computational and Applied Mathematics (2019), https://doi.org/10.1016/j.cam.2019.04.028.

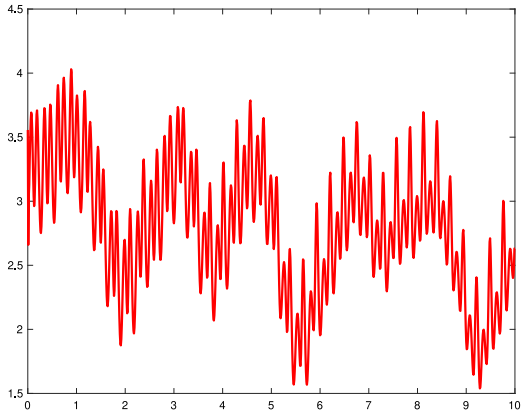

Fig. 8. Example 5 signal.

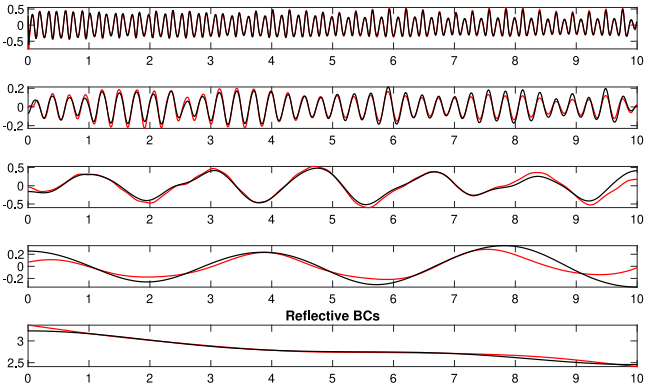

Fig. 9. Example 5: decomposition computed by DIF method with Reflective BCs (black line) compared with the exact one (red line). (For interpretation of the references to color in this figure legend, the reader is referred to the web version of this article.)

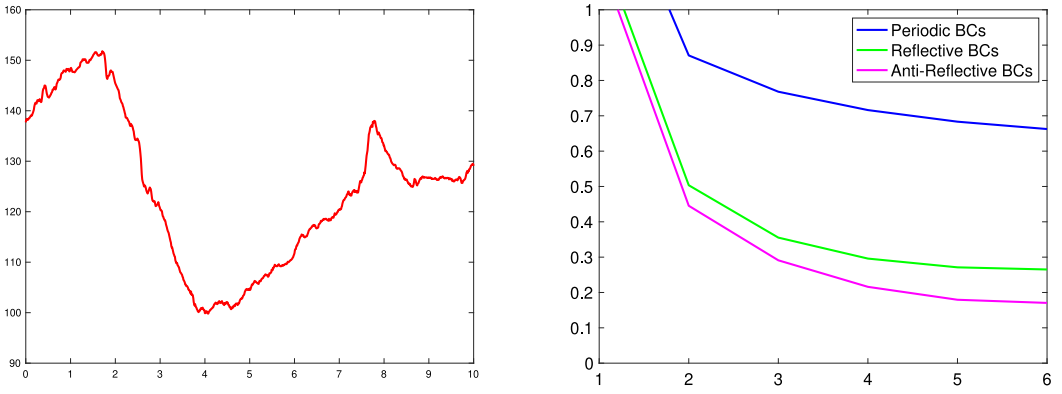

Fig. 10. Left panel: Example 6 signal. Right panel: relative error associated with DIF for different BCs when the number of steps increases.

Conclusions

In this work we study the Iterative Filtering (IF) algorithm for the decomposition of nonstationary signals when Periodic, Reflective and Anti-Reflective boundary conditions (BCs) are employed. Each BC gives rise to a different matrix structure associated with the algorithm. In this paper we analyze the spectral properties of these matrices and the convergence properties of the corresponding method.

Furthermore, we propose an Extended version of IF (EIF), in which any BCs can be employed, and also different BCs for each boundary. This newly defined version of the method allows to estimate the error propagating from the boundary

Please cite this article as: A. Cicone and P. Dell'Acqua, Study of boundary conditions in the Iterative Filtering method for the decomposition of nonstationary signals, Journal of Computational and Applied Mathematics (2019), https://doi.org/10.1016/j.cam.2019.04.028.

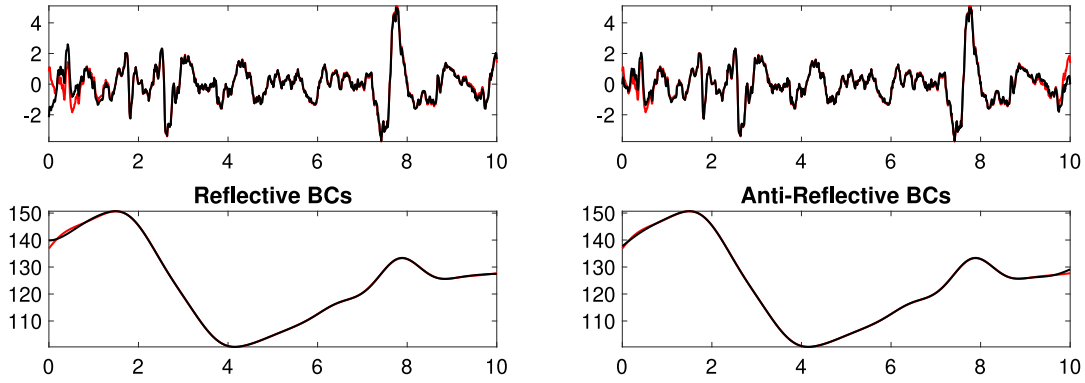

Fig. 11. Example 6 Decomposition computed by DIF method (black line) compared with the exact one (red line), employing Reflective BCs (on the left) and Anti-Reflective BCs (on the right). (For interpretation of the references to color in this figure legend, the reader is referred to the web version of this article.)

towards the internal part of the signal due to the artificial extension of the signal itself. Based on this estimate, we propose a formula which allows to give a priori upper bound for the error which propagates at each iteration inside the IMFS produced using the IF method.

Numerical experiments show that a suitable choice of BCs is able to improve the quality of the decomposition of a given signal computed by the IF method. Furthermore these examples show that the proposed a priori error upper bound is effective in estimating the error induced in the iterations by the extension at the boundaries. This upper bound estimate is far from being tight. It would be extremely valuable for real life applications to develop tighter upper bounds.

Finally we point out that it would be interesting to study new accurate BCs based on the signal at hand, as done in [16,17] for image restoration problem. We plan to work in this direction in the next future.

Acknowledgments

This work was supported by the Istituto Nazionale di Alta Matematica (INdAM) "INdAM Fellowships in Mathematics and/or Applications cofunded by Marie Curie Actions", FP7-PEOPLE-2012-COFUND, Grant Agreement No. PCOFUND-GA-2012-600198.

Some results presented in this paper rely on data collected by one of the three satellites of the Swarm constellation. We thank the European Space Agency (ESA) that supports the Swarm mission. Swarm data can be accessed online at http://earth.esa.int/swarm.

References

[1] N.E. Huang, Z. Shen, S.R. Long, M.C. Wu, H.H. Shih, Q. Zheng, N.C. Yen, C.C. Tung, H.H. Liu, The empirical mode decomposition and the Hilbert spectrum for nonlinear and non-stationary time series analysis, Proc. R. Soc. Lond. Ser. A Math. Phys. Eng. Sci. 454 (1998) 903.
[2] Z. Wu, N.E. Huang, Ensemble empirical mode decomposition: A noise-assisted data analysis method, Adv. Adapt. Data Anal. 1 (2009) 1–41.
[3] L. Lin, Y. Wang, H. Zhou, Iterative filtering as an alternative algorithm for empirical mode decomposition, Adv. Adapt. Data Anal. 1 (2009) 543–560.
[4] A. Cicone, J. Liu, H. Zhou, Adaptive local iterative filtering for signal decomposition and instantaneous frequency analysis, Appl. Comput. Harmon. Anal. 41 (2016) 384–411, http://dx.doi.org/10.1016/j.acha.2016.03.001.
[5] C. Huang, L. Yang, Y. Wang, Convergence of a convolution-filtering-based algorithm for empirical mode decomposition, Adv. Adapt. Data Anal. 1 (2009) 561–571.
[6] A. Cicone, H. Zhou, Iterative Filtering algorithm numerical analysis with new efficient implementations based on FFT, submitted for publication. ArXiv:1802.01359.
[7] A. Cicone, H. Zhou, Multidimensional iterative filtering method for the decomposition of high-dimensional non-stationary signals, Numer. Math. Theory Methods Appl. 10 (2017) 278–298, http://dx.doi.org/10.4208/nmtma.2017.s05.
[8] A. Cicone, Iterative Filtering as a direct method for the decomposition of nonstationary signals, submitted for publication. ArXiv:1811.03536.
[9] A. Cicone, Multivariate Fast Iterative Filtering for the decomposition of nonstationary signals, submitted for publication. ArXiv:1902.04860.
[10] A. Cicone, J. Liu, H. Zhou, Hyperspectral chemical plume detection algorithms based on multidimensional iterative filtering decomposition, Philos. Trans. R. Soc. Lond. Ser. A Math. Phys. Eng. Sci. 374 (2016) 20150196, http://dx.doi.org/10.1098/rsta.2015.0196.
[11] A. Cicone, C. Garoni, S. Serra-Capizzano, Spectral and convergence analysis of the Discrete ALIF method, To appear on Linear Algebra and Its Applications. http://www.it.uu.se/research/publications/reports/2017-018/.
[12] A. Cicone, Nonstationary signal decomposition for dummies, in: Advances in Mathematical Methods and High Performance Computing, in: Advances in Mechanics and Mathematics, vol. 41, Springer Nature, 2019, http://dx.doi.org/10.1007/978-3-030-02487-1, Chapter 3.
[13] P. Dell'Acqua, M. Donatelli, S. Serra-Capizzano, D. Sesana, C. Tablino-Possio, Optimal preconditioning for image deblurring with Anti-Reflective boundary conditions, Linear Algebra Appl. 502 (2016) 159–185.
[14] P. Dell'Acqua, M. Donatelli, C. Estatico, M. Mazza, Structure preserving preconditioners for image deblurring, J. Sci. Comput. 72 (2017) 147–171.
[15] P. Dell'Acqua, M. Donatelli, L. Reichel, Non-stationary structure-preserving preconditioning for image restoration, submitted for publication.
[16] P. Dell'Acqua, A note on Taylor boundary conditions for accurate image restoration, Adv. Comput. Math. 43 (2017) 1283–1304.

[17] P. Dell'Acqua, F. Durastante, New periodicontinuous boundary conditions for fast and accurate image restoration, submitted for publication.
[18] N.E. Huang, S.S. Shen, Hilbert–Huang Transform and Its Applications, World Scientific, 2005.
[19] R.T. Rato, M.D. Ortigueira, A.G. Batista, On the HHT, its problems, and some solutions, Mech. Syst. Signal Process. 22 (2008) 1374–1394.
[20] M.K. Ng, R.H. Chan, W.C. Tan, A fast algorithm for deblurring models with Neumann boundary conditions, SIAM J. Sci. Comput. 21 (1999) 851–866.
[21] S. Serra Capizzano, A note on antireflective boundary conditions and fast deblurring models, SIAM J. Sci. Comput. 25 (2003) 1307–1325.
[22] A. Aricò, M. Donatelli, J. Nagy, S. Serra-Capizzano, The Anti-Reflective transform and regularization by filtering, numerical linear algebra in signals, Syst. Control (2011) 1–21.
[23] M. Donatelli, S. Serra Capizzano, On the treatment of boundary artifacts in image restoration by reflection and/or anti-reflection, in: V. Olshevsky, E. Tyrtyshnikov (Eds.), Matrix Methods: Theory, Algorithms and Applications, World Scientific, 2010, pp. 227–237.

Please cite this article as: A. Cicone and P. Dell'Acqua, Study of boundary conditions in the Iterative Filtering method for the decomposition of nonstationary signals, Journal of Computational and Applied Mathematics (2019), https://doi.org/10.1016/j.cam.2019.04.028.